J Bioenerg Biomembr (2008) 40:607–618
DOI 10.1007/s10863-008-9188-0

Role of reactive oxygen species-mediated mitochondrial dysregulation in 3-bromopyruvate induced cell death in hepatoma cells

ROS-mediated cell death by 3-BrPA

Ji Su Kim · Keun Jae Ahn · Jeong-Ah Kim · Hye Mi Kim · Jong Doo Lee · Jae Myun Lee · Se Jong Kim · Jeon Han Park

Received: 5 June 2008 / Accepted: 4 November 2008 / Published online: 6 December 2008

Abstract Hexokinase type II (HK II) is the key enzyme for maintaining increased glycolysis in cancer cells where it is overexpressed. 3-bromopyruvate (3-BrPA), an inhibitor of HK II, induces cell death in cancer cells. To elucidate the molecular mechanism of 3-BrPA-induced cell death, we used the hepatoma cell lines SNU449 (low expression of HKII) and Hep3B (high expression of HKII). 3-BrPA induced ATP depletion-dependent necrosis and apoptosis in both cell lines. 3-BrPA increased intracellular reactive oxygen species (ROS) leading to mitochondrial dysregulation. NAC (*N*-acetyl-L-cysteine), an antioxidant, blocked 3-BrPA-induced ROS production, loss of mitochondrial membrane potential and cell death. 3-BrPA-mediated oxidative stress not only activated poly-ADP-ribose (PAR) but also translocated AIF from the mitochondria to the nucleus. Taken together, 3-BrPA induced ATP depletion-dependent necrosis and apoptosis and mitochondrial dysregulation due to ROS production are involved in 3-BrPA-induced cell death in hepatoma cells.

Keywords 3-bromopyruvate · ATP depletion-dependent necrosis · Apoptosis · ROS · Mitochondrial dysregulation

Abbreviations

AIF	Apoptosis inducing factor
3-BrPA	3-bromopyruvate
HK II	Hexokinase isoenzyme type II
MMP	Mitochondrial membrane potential
NAC	*N*-acetyl-L-cysteine
PAR	Poly-ADP-ribose
PARP	Poly(ADP-ribose) polymerase
ROS	Reactive oxygen species

Introduction

Glucose is critical both as an energy source to maintain cell survival and as a carbon source for cell building blocks.

J. S. Kim · J. M. Lee · S. J. Kim · J. H. Park (✉)
Department of Microbiology and Brain Korea 21 Project for Medical Sciences, Institute for Immunology and Immunological Diseases, Yonsei University College of Medicine,
134, Shinchon-dong, Seodaemoon-gu,
120-752 Seoul, South Korea
e-mail: jhpark5277@yuhs.ac

K. J. Ahn · J. D. Lee
Division of Nuclear Medicine, Department of Diagnostic Radiology, Yonsei University College of Medicine,
Seoul, South Korea

J.-A. Kim
Department of Radiology, Cheil General Hospital and Women's Healthcare Center, Kwandong University College of Medicine,
Seoul, South Korea

H. M. Kim
Department of Diagnostic Radiology,
Yonsei University College of Medicine,
Seoul, South Korea

Present address:
J. S. Kim
Yonsei Cancer Research Institute,
Yonsei University College of Medicine,
Seoul, South Korea

Present address:
J.-A. Kim
Department of Radiology, Yongdong Severance Hospital,
Yonsei University College of Medicine,
Seoul, South Korea

Many cancer cells have aberrant energy metabolism in which they consume more glucose than normal cells and rapidly convert it to lactate. The elevated glucose catabolism in tumors is known as the Warburg effect. Hexokinase (HK) is essential for maintaining the high rate of glycolysis in these cells. Of the four HKs, HK I, HK II, HK III, and HK IV (glucokinase), HK II is known to play a major role in sustaining a highly malignant state (Mathupala et al. 1995; Mathupala et al. 2006). HK II is overexpressed in many tumor cell types leading to an increase in adenosine triphosphate (ATP) production (Chang et al. 2007). In addition, HK II has been reported to suppress the death of cancer cells by binding mitochondria through an interaction with a voltage dependent anion channel (VDAC) that regulates the entry of intermembrane space proteins including cytochrome *c* and apoptosis inducing factor (AIF) into the cytosol during cell death (Pastorino et al. 2005).

Mitochondria are important in the control of both cell survival and cell death. Mitochondrial dysregulations, such as loss of trans-membrane potential, accumulation of reactive oxygen species (ROS), membrane permeability transition and release of pro-apoptotic factors lead to apoptosis or necrosis (Higuchi 2004). Mitochondria are the specialized redox-active organelles that control cell death associated with ROS production (McEligot et al. 2005). When ROS concentrations reach a certain threshold level, the antioxidant defense is overwhelmed leading to oxidative stress (Kakkar and Singh 2007). Since redox sensitive caspase activity and cytochrome *c* release are dependent on the intracellular redox state, this modulates the cellular morphologic changes, whether it be apoptosis or necrosis (Ueda et al. 2002). ROS induce both DNA strand breaks and activation of the nuclear enzyme poly(ADP-ribose) polymerase-1 (PARP-1) (van Wijk and Hageman 2005). Cells that utilize almost exclusively glucose via glycolysis and oxidative phosphorylation die from NAD^+ and ATP depletion as a consequence of PARP-1 activation. PARP-1 is one substrate for caspase-3 and is controlled by caspase-3 activity. Recently it was reported that the specific PARP-1-mediated caspase-independent cell death pathway leads to release of AIF from the mitochondria to the cytosol (Otera et al. 2005) and the nucleus (Yu et al. 2002).

3-bromopyruvate (3-BrPA) is a strong alkylating agent. It inhibits both HK II and mitochondrial oxidative phosphorylation, leading to decreased ATP production which, in turn, leads to cell death (Foubister 2002; Ko et al. 2001). 3-BrPA plays an important role in killing liver cancer cells by local infusion in the VX2 tumor implantation animal tumor model (Geschwind et al. 2002). In an animal model with advanced cancers, 3-BrPA therapy to deplete ATP selectively destroyed them without apparent toxicity or recurrence (Ko et al. 2004). Necrosis results from energy catabolism perturbation upon ATP depletion by 3-BrPA as ATP depletion is one of the causes of necrosis (Lemasters 2005). It was also demonstrated that 3-BrPA induced apoptosis in human leukemia and lymphoma cell lines, in which the pro-apoptotic protein Bad was dephosphorylated, and Bax was translocated from the cytosol to the mitochondria leading to the activation of the executioner caspase, caspase-3 (Xu et al. 2005). Although 3-BrPA has been reported to have an anti-cancer effect (Ko et al. 2001), the molecular mechanism of cell death induced by 3-BrPA is not clear.

To investigate the molecular mechanism of 3-BrPA-induced cell death, we studied the effect of 3-BrPA on cell death in hepatoma cell lines with different expression levels of HK II. Based on our results, we suggest that 3-BrPA induces ATP depletion-dependent necrosis and apoptosis together with ROS generated by 3-BrPA leading to loss of mitochondrial regulation. This in turn, leads to poly-ADP-ribose (PAR) activation and AIF translocation to the nucleus which might be involved in part in 3-BrPA-induced cell death in hepatoma cells independent of their expression levels of HK II.

Materials and methods

Cell culture

The human hepatocellular carcinoma cell line Hep3B (ATCC HB 8064) was obtained from the ATCC (Rockville, MD, USA). SNU449 was obtained from the Korean Cell Line Bank (Seoul, Korea) (Park et al. 1995). Cells were grown in modified Eagle's medium (MEM) (GIBCO BRL, Grand Island, NY, USA) supplemented with 10% fetal bovine serum (GIBCO BRL), 2 mM glutamine, 100 U/ml penicillin and 100 μg/ml streptomycin at 37 °C in an atmosphere containing 5% CO_2.

Reagents

3-BrPA was obtained from Sigma-Aldrich, Inc. (St. Louis, MO, USA). The 3-BrPA solution was prepared as described (Geschwind et al. 2002). Briefly, the compound was freshly dissolved into PBS, pH 7.5 and neutralized with NaOH immediately before use. *N*-acetyl-L-cysteine (NAC) was purchased from Calbiochem (La Jolla, CA, USA). Dichlorodihydrofluorescein diacetate (H_2DCFDA) and 5,5′,6,6′-tetrachloro-1,1′,3,3′-tetraethylbenzimidazolyl-carbocyanine iodide (JC-1) were obtained from Molecular Probes (Eugene, OR, USA). Rabbit anti-caspase-3 and anti-PARP antibodies were purchased from Cell signaling Technology, Inc. (Beverly, MA, USA). Mouse anti-cytochrome *c* antibody was purchased from Pharmingen (San Diego, CA, USA). Mouse anti-HSP60 was purchased from Santa Cruz Bio Technology (Santa Cruz, CA, USA). Mouse anti-α tubulin antibody was

purchased from Oncogene Research Products (Boston, MA, USA). Rabbit anti-caspase-9 and anti-PAR antibodies were obtained from Pharmingen. Rabbit anti-HK II and anti-AIF antibodies were purchased from Chemicon (Temecula, CA, USA) and Serotec (Kidlington, Oxford, UK), respectively.

RT-PCR

Total RNA was isolated using an RNeasy kit (Qiagen, Santa Clarita, CA, USA). cDNA was synthesized by reverse transcription with 5 μg total RNA, 0.5 μg of random hexamer (Promega, Madison, WI, USA), 1.25 mM dNTP (Boehringer Mannheim, Mannheim, Germany) and 200 U MMLV-RT (GIBCO BRL) in a 20 μl reaction. PCR was performed with 3 μl cDNA, 10 pmol of primer sets, 0.25 mM dNTP and 2 U Taq polymerase (Perkin Elmer, Norwalk, CT, USA). PCR cycling conditions were as follows: 23–35 cycles of denaturation at 94 °C for 30 s, annealing at 56–60 °C for 30 s, and extension at 72 °C for 30 s. The sequences of primers were as follows: *HKII*, (sense) 5′-AGTGGAGTGGAAGGCA GAGA-3′ and (antisense) 5′-CGCATCTCTTCCATGT AGCA-3′; and *GAPDH*, (sense) 5′-TGATGACATCAAGAA GGTGGTGAAG-3′ and (antisense) 5′-TCCTTGGAGGCC ATGTGGGCCAT-3′. The PCR products were analyzed by agarose gel electrophoresis.

Cell viability assay and measurement of intracellular ATP levels

Cell viability was analyzed by the 3-(4,5-dimethylthiazol-2-yl)-2,5-diphenyltetrazolium bromide (MTT) assay. Briefly, cells were seeded to a 96-well plate in 100 μl medium, left overnight to adhere, and cells were treated with various concentrations of 3-BrPA for different time periods. After treatment, 50 μl of MTT solution (2 mg/ml in PBS) was added to each well and incubated for another 4 h at 37 °C. The plates were then centrifuged at 1,200×g for 10 min, the supernatant was discarded and 50 μl dimethylsulfoxide (DMSO) was added to each well. Plates were then shaken until the crystals were dissolved. Reduced MTT was measured spectrophotometrically in a beam microplate reader (Molecular Devices, Toronto, Canada) at 570 nm.

Intracellular ATP levels were measured using CellTiter-Glo® Luminescent Cell Viability Assay (Promega) according to the manufacturer's instructions. Briefly, cells were cultured as above and treated with 100 μM 3-BrPA for different time periods. Then, the CellTiter-Glo kit agent was added in aliquots of 100 μl and incubated for 30 min. The luminescence produced by the luciferase-catalyzed luciferin plus ATP reaction was detected using a MicroLumat LB96P multiwell scanning spectrophotometer (EG&G Berthold, Bad Wildbad, Germany). The data were normalized to the control group.

Annexin V and propidium iodide staining

To measure cell death, Annexin V and propidium iodide (PI) staining were performed using an Annexin V-FITC Apoptosis Kit (BioSource, Camarillo, CA, USA). Briefly, after treatment with 100 μM 3-BrPA, cells were washed twice with PBS, collected and resuspended in 100 μl of 1× Annexin V-FITC binding buffer. Five microliters of Annexin V-FITC conjugate and 10 μl PI buffer were added, and the cells were incubated at room temperature for 15 min in the dark. After adding 400 μl of 1× Annexin V-FITC binding buffer, the cells were analyzed using a FACScan flow cytometer (Becton Dickinson, San Jose, CA, USA).

Determination of mitochondrial membrane potential ($\Delta\varphi_m$)

To detect $\Delta\varphi_m$ changes, cells (2×10^5 cells/well) treated with 100 μM 3-BrPA were harvested at the indicated time points and stained with 10 μg/ml JC-1 for 10 min at room temperature in the dark. Stained cells were washed twice with cold PBS and resuspended in 400 μl PBS for flow cytometry.

Detection of ROS production

To assay ROS production, cells were stained with 4 μM chloromethyl-2,7-dichlorodihydrofluorescein diacetate (CM-H_2DCFDA, Molecular Probes), at 37 °C for 30 min. After incubation with CM-H_2DCFDA, which is oxidized to dichlorofluorescein (DCF) by ROS, cells were treated with 100 μM 3-BrPA, washed, and detached with trypsin. After centrifugation, ROS generation was immediately determined by FACS analysis.

Separation of the cytosolic and mitochondrial proteins

Cytosolic and mitochondrial proteins were separated as described previously (Kim et al. 2004). Briefly, cells treated with 100 μM 3-BrPA were collected and suspended in mitochondria isolation buffer (20 mM Hepes-KOH, pH 7.5, 210 mM sucrose, 70 mM mannitol, 1 mM EDTA, 1 mM DTT, 1.5 mM $MgCl_2$, 10 mM KCl) and protease inhibitor cocktail (Boehringer Mannheim) supplemented with 10 mM digitonin (Sigma-Aldrich Co.). Suspensions were incubated at 37 °C for 10 min and centrifuged at 12,000×*g* for 15 min. The supernatant (cytosolic fraction) and pellet containing the mitochondria were collected for western blot analysis.

Preparation of nuclear proteins

The cells were washed with ice-cold PBS and resuspended in a nuclear extraction buffer A (10 mM HEPES, pH 7.9,

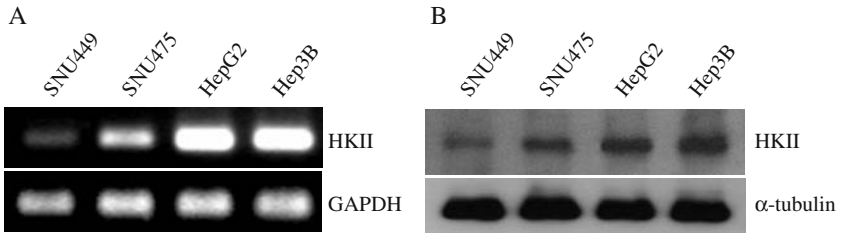

Fig. 1 The expression of HK II in hepatoma cells. For the detection of endogenous HK II mRNA and protein in a panel of hepatoma cell lines, RT-PCR (**a**) was performed with the HK II primer set, and Western blot analysis (**b**) was carried out in a panel of hepatoma cell lines

10 mM KCl, 0.1 mM EDTA, 0.1 mM EGTA, 1 mM DTT, 0.5 mM PMSF). After 0.1% NP-40 addition, the suspensions were vigorously vortexed and then centrifuged at 12,000×g for 30 s. The nuclear pellet was resuspended in nuclear extraction buffer C (20 mM HEPES, pH 7.9, 0.4 M KCl, 1 mM EDTA, 1 mM EGTA, 1 mM DTT, 1 mM PMSF). After vigorous rocking, suspensions were incubated at 4 °C for 15 min and centrifuged at 12,000×*g* for 15 min. The supernatant (nuclear fraction) was collected for western blot analysis.

Western blot analysis

After 3-BrPA treatments, cells were lysed in RIPA buffer (50 mM Tris–HCl, pH 7.4, 0.5 mM EDTA, 1.8 μg/ml aprotinin, 100 mM NaCl, 0.2% NP-40, 2 mM $MgCl_2$, 0.5 mM PMSF), and the lysates were cleared by centrifugation at 15,000 rpm for 15 min. One hundred micrograms of cell lysates were used for 8–12% SDS-PAGE, which was followed by western blotting using the appropriate antibodies. Proteins were visualized by Western Blotting Luminol Reagent (Amersham Pharmacia Biotech, Piscataway, NJ, USA).

Results

3-BrPA induces ATP depletion-dependent necrotic and caspase-independent apoptotic cell death

To determine whether 3-BrPA-induced cell death in hepatoma cell lines is related to the endogenous expression levels of HK II, the endogenous expression levels of HK II were screened by RT-PCR and western blot analysis in a panel of hepatoma cell lines, SNU449, SNU475, HepG2, and Hep3B. Expression levels of HK II were varied; SNU449 displayed low level of expression, SNU475 showed a moderate level of expression, and HepG2 and Hep3B cells both had high levels of expression (Fig. 1a and b). SNU449 and Hep3B cells were used for further study.

To determine the effect of 3-BrPA on cell viability of SNU449 and Hep3B cells, cells were treated with different concentrations of 3-BrPA at various time intervals and the MTT assay was performed. Although both cell lines were sensitive to 3-BrPA at high concentrations (200 μM), Hep3B cells were more sensitive than SNU449 cells at the 50–100 μM 3-BrPA range over 6 h (Fig. 2a).

3-BrPA inhibits both glycolysis and mitochondria ATP production causing ATP depletion (Ko et al. 2004) that leads to ATP depletion-dependent necrotic cell death. However, 3-BrPA was also known to activate mitochondrial apoptotic signaling cascades such as release of cytochrome *c*, Smac/DIABLO, AIF, and activation of caspase-3 leading to apoptosis (Gwak et al. 2005), and it was recently reported to induce necrosis as well as apoptosis in VX-2 tumors (Vali et al. 2007).

To elucidate the cell death mechanism induced by 3-BrPA in hepatoma cells, measurements of intracellular ATP levels and a cell death assay with Annexin V-FITC and PI staining were performed. Treatment of cells with 100 μM 3-BrPA for 24 h led to an approximately 60% decrease in intracellular ATP levels in both cell lines (Fig. 2b). PI single-positive and Annexin V-PI dual-positive cell populations started to appear as early as 1 h (Fig. 2c) indicating that 3-BrPA induces rapid cell death by both necrosis and apoptosis. To further elucidate the apoptotic cell death mechanism induced by 3-BrPA in hepatoma cells, cleavages of procaspase-3 and PARP-1 were analyzed by western blotting. At indicated time points, the active forms of cleaved caspase-3 and the p89 cleavage product of PARP-1 were not detected in 3-BrPA treated cells (Fig. 3a) compared with Hep3B cells treated with cisplatin as a positive control (Kim et al. 2004). To confirm caspase-independent apoptosis by 3-BrPA, a pan caspase inhibitor, z-VAD-fmk, was pretreated. z-VAD-fmk did not block 3-BrPA-induced cell death (Fig. 3b). These data suggest that 3-BrPA induces cell death

Fig. 2 3-BrPA induced cell death in hepatoma cell lines. **a** After cells were treated with different concentrations of 3-BrPA at various time intervals, the effect of 3-BrPA on cell viability was determined by the MTT assay. **b** After cells were treated with 100 μM 3-BrPA at various time intervals, the effect of 3-BrPA on intracellular ATP levels was determined by CellTiter-Glo® Luminescent Cell Viability Assay kit (Promega). **c** After cells were treated with 100 μM 3-BrPA at various time intervals, the effect of 3-BrPA on cell death was quantitatively measured with Annexin V-FITC (*X* axis) and PI (*Y* axis) and analyzed by flow cytometry. The data shown are representative of three independent experiments. *UT* untreated, *3-Br* 3-bromopyruvate treated

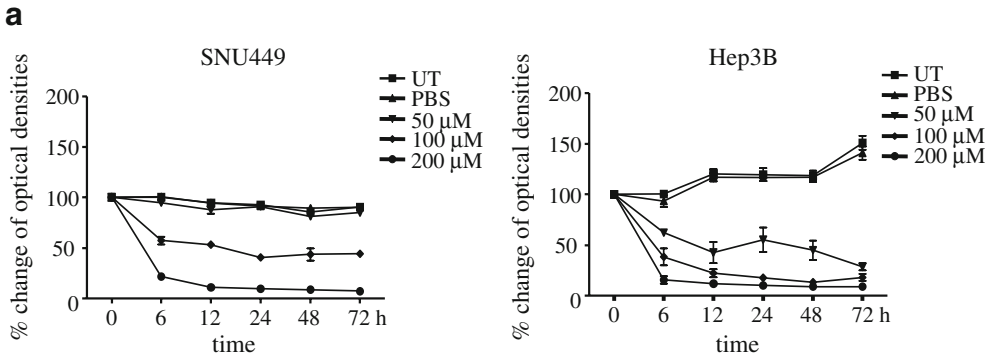
a
SNU449
Hep3B
% change of optical densities
200
150
100
50
0
0 6 12 24 48 72 h
time
UT
PBS
50 μM
100 μM
200 μM

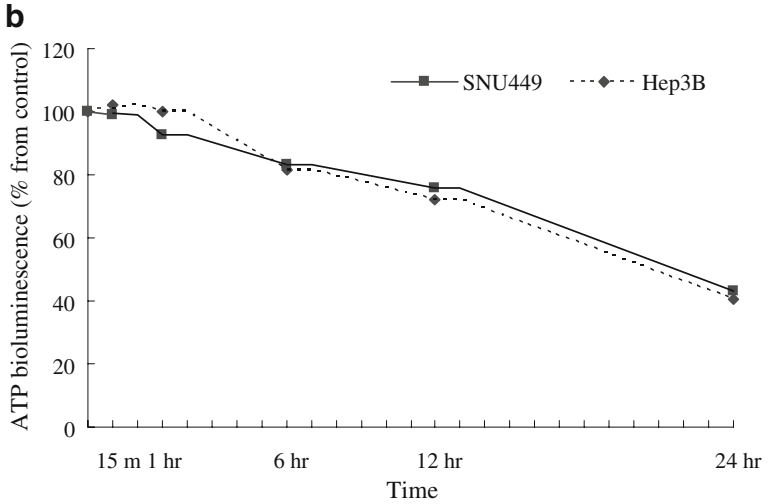
b
ATP bioluminescence (% from control)
120
100
80
60
40
20
0
SNU449
Hep3B
15 m 1 hr
6 hr
12 hr
24 hr
Time

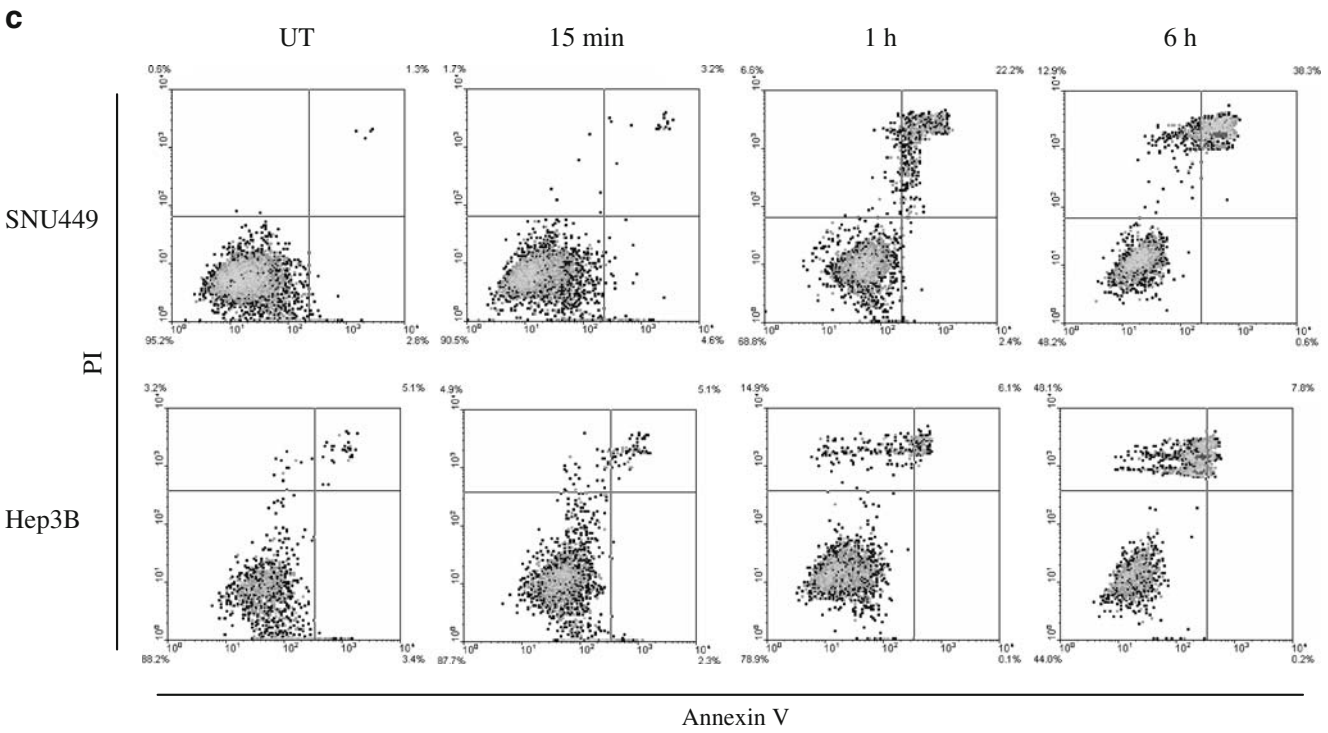
c
UT
15 min
1 h
6 h
SNU449
Hep3B
PI
Annexin V

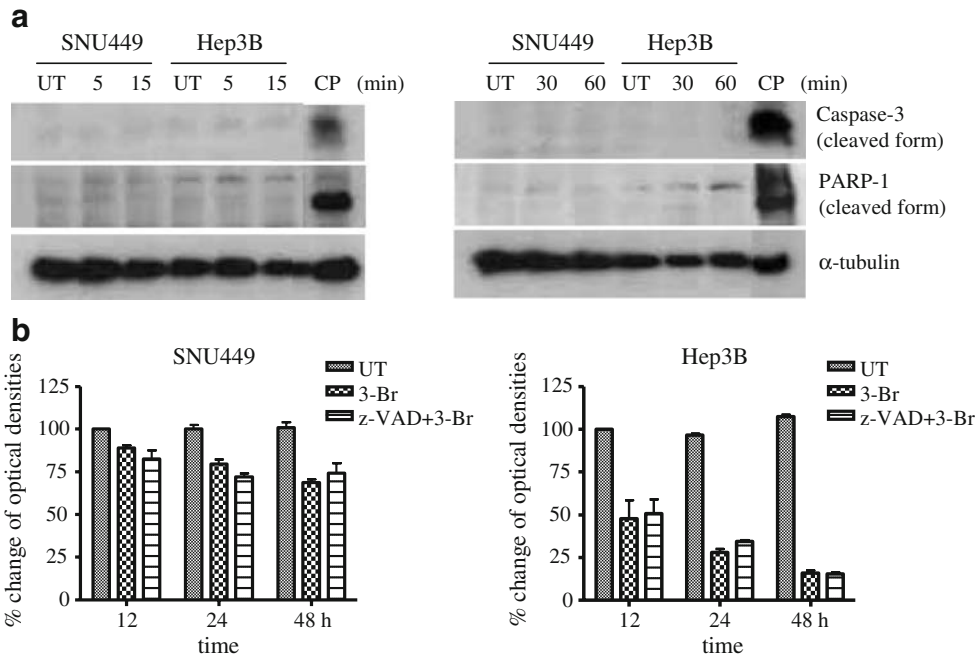

Fig. 3 3-BrPA activates a caspase-independent apoptotic cell death pathway. **a** Cells were treated with 100 μM 3-BrPA and harvested at indicated time points. Cell lysates were analyzed by Western blot using antibodies specific for the active forms of caspase-3, PARP-1, and α-tubulin, respectively. **b** Cells were pretreated with 100 μM z-VAD-fmk for 1 h followed by treatment with 100 μM 3-BrPA. The effect of z-VAD-fmk on 3-BrPA-induecd cell death was analyzed by MTT assay

via both an ATP depletion-dependent necrotic and a caspase-independent apoptotic cell death pathway.

3-BrPA induces ROS production and mitochondrial dysregulation

It has been reported that ROS generation induces apoptosis as well as necrosis followed by mitochondrial dysregulation, including mitochondrial matrix swelling, loss of MMP, and giant DNA fragments (Higuchi 2004). To investigate the accumulation of intracellular ROS, 3-BrPA-treated cells were labeled with CM-H_2DCFDA, a cell permeable fluorescent dye, and analyzed by FACS. 3-BrPA-induced ROS production was detected at 15 min and remained until 1 h in both SNU449 and Hep3B cells (Fig. 4a). 3-BrPA-induced ROS generation was more prominent in SNU449 than Hep3B cells. Since ROS-mediated cell death is related to mitochondrial dysregulation, we analyzed MMP with JC-1 staining. The loss of MMP was found in a time-dependent manner in both cell lines (Fig. 4b) indicating that 3-BrPA induced ROS production leads to mitochondrial dysregulation but is not related to the expression level of HK II.

The effect of an antioxidant on 3-BrPA-induced cell death

To investigate whether ROS play an essential role in 3-BrPA-induced cell death, we examined the effect of an antioxidant, NAC, on 3-BrPA-induced cell death. Cells were pretreated with various concentrations of NAC before 3-BrPA treatments, and an MTT assay was performed. Pretreatment with NAC did not affect cell viability and inhibited 3-BrPA-induced cell death at a 2 mM concentration (Fig. 5a). We also performed vice versa, i.e., 2 mM NAC was added at the same time or after treatment of cells with 3-BrPA for 15 min, because 3-BrPA-induced ROS production was detected from 15 min as shown in Fig. 4a. Then an Annexin V-PI staining was performed. Addition of NAC also inhibited 3-BrPA-induced cell death (Fig. 5b). In addition, NAC did not have an effect on intracellular ROS levels, but it completely blocked 3-BrPA-induced ROS production in both cell lines (Fig. 5c). We investigated whether 3-BrPA-induced oxidative stress following ROS production was critical in the loss of MMP. Addition of NAC completely suppressed 3-BrPA-induced loss of MMP (Fig. 5d), implying that ROS production might act upstream of mitochondrial dysregulation in 3-BrPA-induced cell death in the hepatoma cell lines used in this study.

The effect of 3-BrPA on activation of PARP-1 and translocation of AIF to nucleus

Cytochrome *c* release was determined to further study mitochondrial dysregulation induced by 3-BrPA. After treatment of cells with 3-BrPA, cell lysates were fractionated to cytosolic and mitochondrial proteins, and the cytochrome *c* release from the mitochondria to the cytosol was analyzed using western blot. Release of cytochrome *c* from the mitochondria to the cytosol was detected to some extent in Hep3B cells, but there was no significant cytochrome *c* release in SNU449 cells (Fig. 6a). Cytochrome *c* release from the mitochondria to the cytosol is known to activate the mitochondria related caspases, caspase-9 and -3 (Adrain et al. 2001). In Hep3B cells,

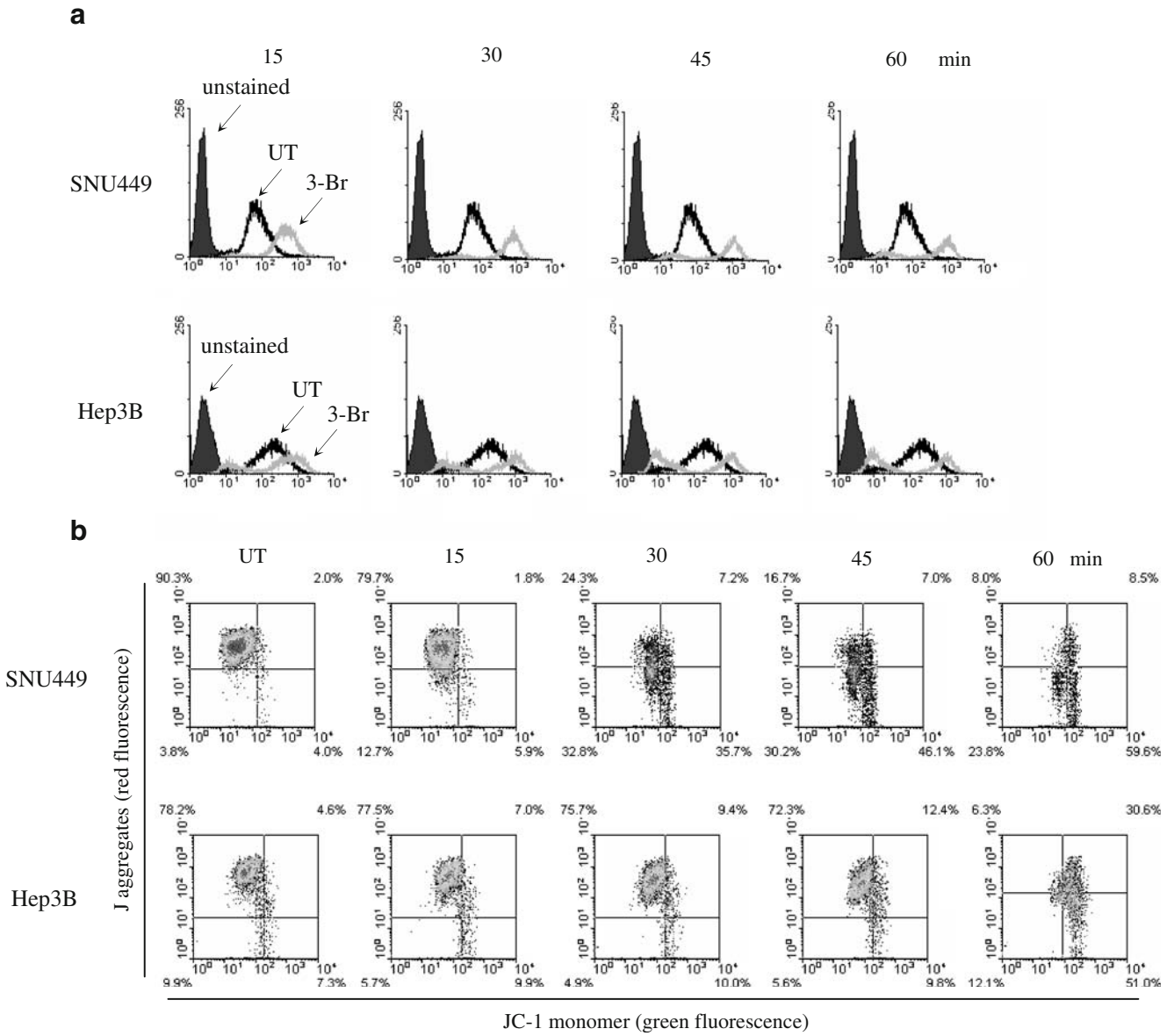

Fig. 4 3-BrPA induced ROS production and mitochondrial dysregulation. **a** Cells were treated with 100 μM 3-BrPA for the indicated time intervals and then stained with 4 μM CM-H_2DCFDA for 30 min. Levels of intracellular ROS were determined by FACS analysis. **b** For the cytofluorometric analysis of $\Delta\varphi_m$, cells treated with 100 μM 3-BrPA were stained with JC-1. Green emission was measured in channel 1 (*X* axis) and red emission in channel 2 (*Y* axis)

although the efflux of cytochrome *c* was detected, there was neither the activation of caspase-9 and -3 nor the cleavage of PARP-1 (Fig. 6b).

It is known that ROS-induced DNA damage activates PARP-1 leading to cell death. Recently, PARP-1-mediated cell death has been reported to have features such as necrosis as well as apoptosis (Kang et al. 2004). To investigate whether PARP-1 activation is involved in 3-BrPA-induced cell death in hepatoma cells, we determined activation of PARP-1 by detecting PAR formation. 3-BrPA activated PARP-1 leads to the formation of PAR in both cell lines (Fig. 6c). Since PARP-1 hyperactivation is known to promote mitochondrial dysregulation leading to release of AIF from the mitochondria to the nucleus (Xu et al. 2006), we investigated whether the release and translocation of AIF from the mitochondria to the nucleus are induced in 3-BrPA treated cells. In spite of inactivation of caspase-9 and -3, the expression levels of AIF were increased, and AIF clearly translocated from the mitochondria to the nucleus in both cell lines (Fig. 6d). Taken together, these data suggest that the mechanism of 3-BrPA-induced cell death might be related to the following signals, ATP depletion, ROS production, loss of MMP, PARP-1 hyperactivation, and AIF translocation.

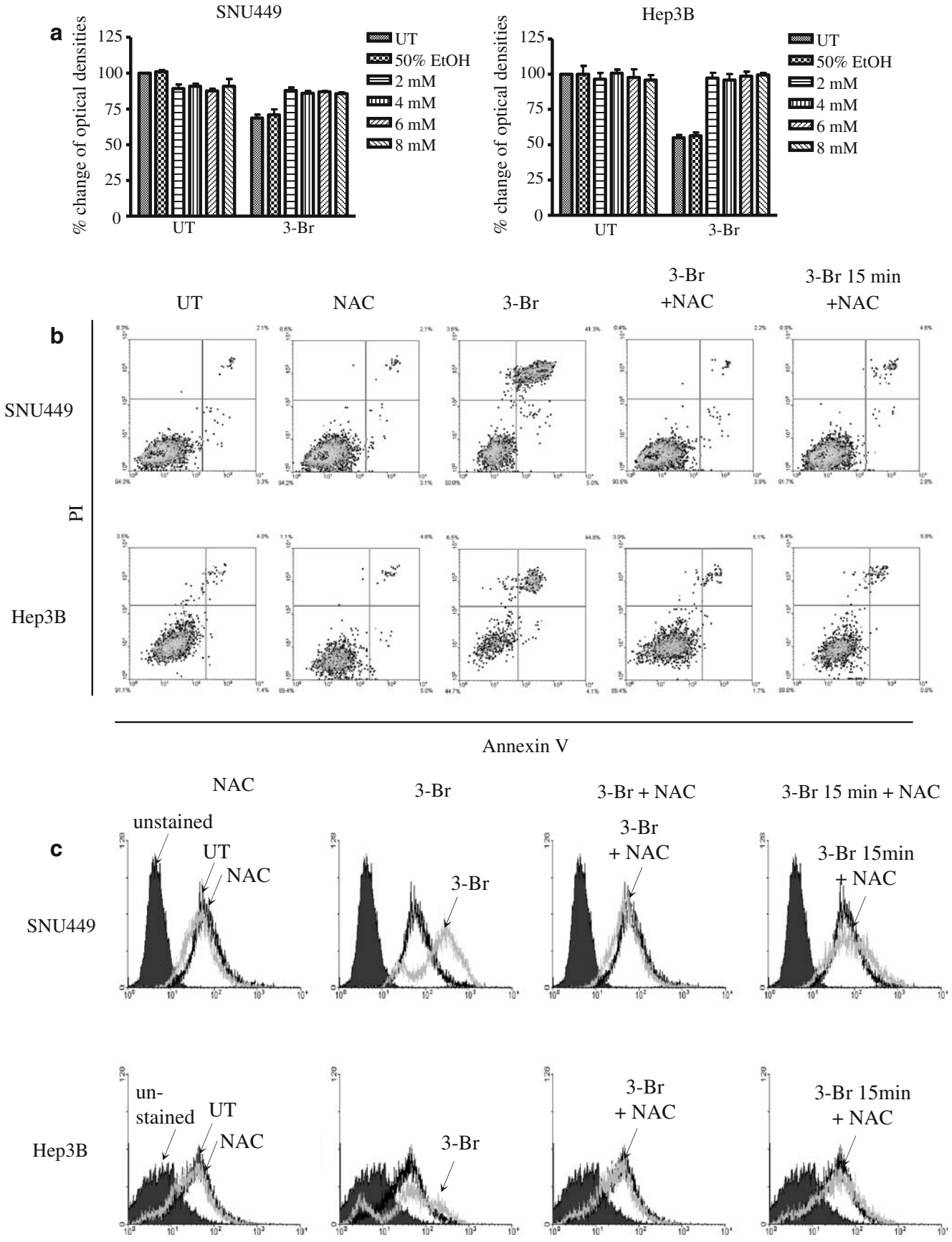
a
SNU449
Hep3B
% change of optical densities
125
100
75
50
25
0
UT
3-Br
UT
50% EtOH
2 mM
4 mM
6 mM
8 mM
b
UT
NAC
3-Br
3-Br +NAC
3-Br 15 min +NAC
SNU449
Hep3B
PI
Annexin V
c
NAC
3-Br
3-Br + NAC
3-Br 15 min + NAC
unstained
UT
NAC
3-Br
3-Br + NAC
3-Br 15min + NAC
un-stained
UT
NAC
3-Br
3-Br + NAC
3-Br 15min + NAC
SNU449
Hep3B

◀**Fig. 5** The effect of an antioxidant, NAC, on 3-BrPA-induced cell death. **a** Cells were pretreated with various concentrations of the antioxidant, NAC for 1 h, followed by a 6 h treatment with 100 μM 3-BrPA. The effect of NAC on 3-BrPA-induced cell death was determined by the MTT assay. Cells treated with 50% ethanol served as controls. **b** The effect of NAC on 3-BrPA-induced cell death was quantitatively measured with Annexin V-FITC (*X* axis) and PI (*Y* axis). NAC (2 mM) was added at the same time (3-Br + NAC) or 15 min after (3-Br 15 min + NAC) treatment of cells with 100 μM 3-BrPA. Cell death was analyzed by FACScan 6 h after addition of NAC. **c** Cells were treated with 2 mM NAC concomitantly (3-Br + NAC) or 15 min after (3-Br 15 min + NAC) treatment with 100 μM 3-BrPA. After 1 h incubation, cells were stained with 4 μM CM-H_2DCFDA for 30 min. Amount of intracellular ROS was determined by FACS analysis. **d** For the analysis of mitochondrial membrane potential, cells were treated with 2 mM NAC concomitantly (3-Br + NAC) or 15 min after (3-Br 15 min + NAC) treatment with 100 μM 3-BrPA After 1 h incubation, cells were stained with JC-1. Green emission was measured in channel 1 (*X* axis) and red emission in channel 2 (*Y* axis)

Discussion

Cancer cells generally catabolize glucose at a higher rate than their non-transformed counterparts. Hexokinase is known as the first step enzyme in glucose metabolism. Among hexokinase isotypes (HK I, II, III, and IV), HK II is the predominantly overexpressed form in tumor cells. It has been shown that HK II is highly expressed in hepatocellular carcinoma (HCC), especially in the presence of hypoxia (Geschwind et al. 2004). It has also been reported that HK II may play an important role in the survival of cancer cells such as advanced infiltrative HCCs and that inhibition of HK II induces cell death by activating mitochondrial pathways (Kim et al. 2007). Therefore, HK II is one of the therapeutic targets in the glycolytic pathway of aggressive tumors (Ko et al. 2001).

3-BrPA, a lactic acid analog, has been known to be a specific inhibitor of HK II leading to inhibition of both glycolysis and mitochondrial ATP production in rapidly growing cancer cells. When hepatoma cells were exposed to 3-BrPA, the cells were sensitized to cell death (Ko et al. 2001). It might be considered that rapid ATP depletion by 3-BrPA in rapidly growing cells leads to necrotic cell death because ATP depletion is one of the causes of necrosis (Lemasters 2005). Previously, 3-BrPA has also been shown to activate caspase-3, to release cytochrome *c*, Smac, and AIF from the mitochondria to the cytosol, and to induce apoptosis, which is partially inhibited by pretreatment of z-VAD-fmk in the Huh-BAT hepatoma cell line (Gwak et al. 2005). It was reported that 3-BrPA induced dephosphorylation of Bad, translocation of Bax from the cytosol to the mitochondria, release of cytochrome *c* from the mitochondria to the cytosol, and activation of caspase-3 leading to apoptosis in the HL-60 leukemia cell line (Xu et al. 2005). Recently, it was also reported that 3-BrPA induced necrosis as well as apoptosis in VX-2 tumors (Vali et al. 2007). Although some studies have demonstrated the effect of 3-BrPA on cell death and suggested its therapeutic effect on cancer treatment, the molecular mechanism of 3-BrPA-induced cell death has not yet been clarified in HCC.

To investigate whether 3-BrPA-induced cell death was related to the expression level of HK II, we screened the endogenous expression level of HK II in several hepatoma cell lines, SNU449, SNU475, HepG2, and Hep3B. It was found that the expression level of HK II is low in SNU449, moderate in SNU475, and high in both HepG2 and Hep3B.

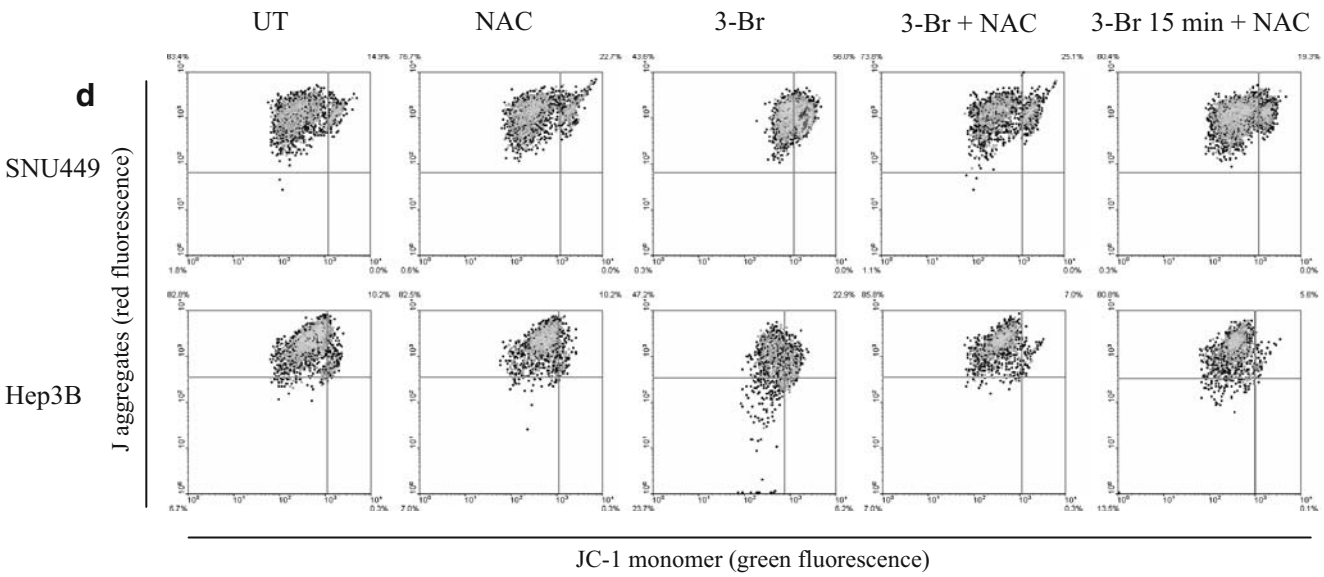

Fig. 5 (continued)

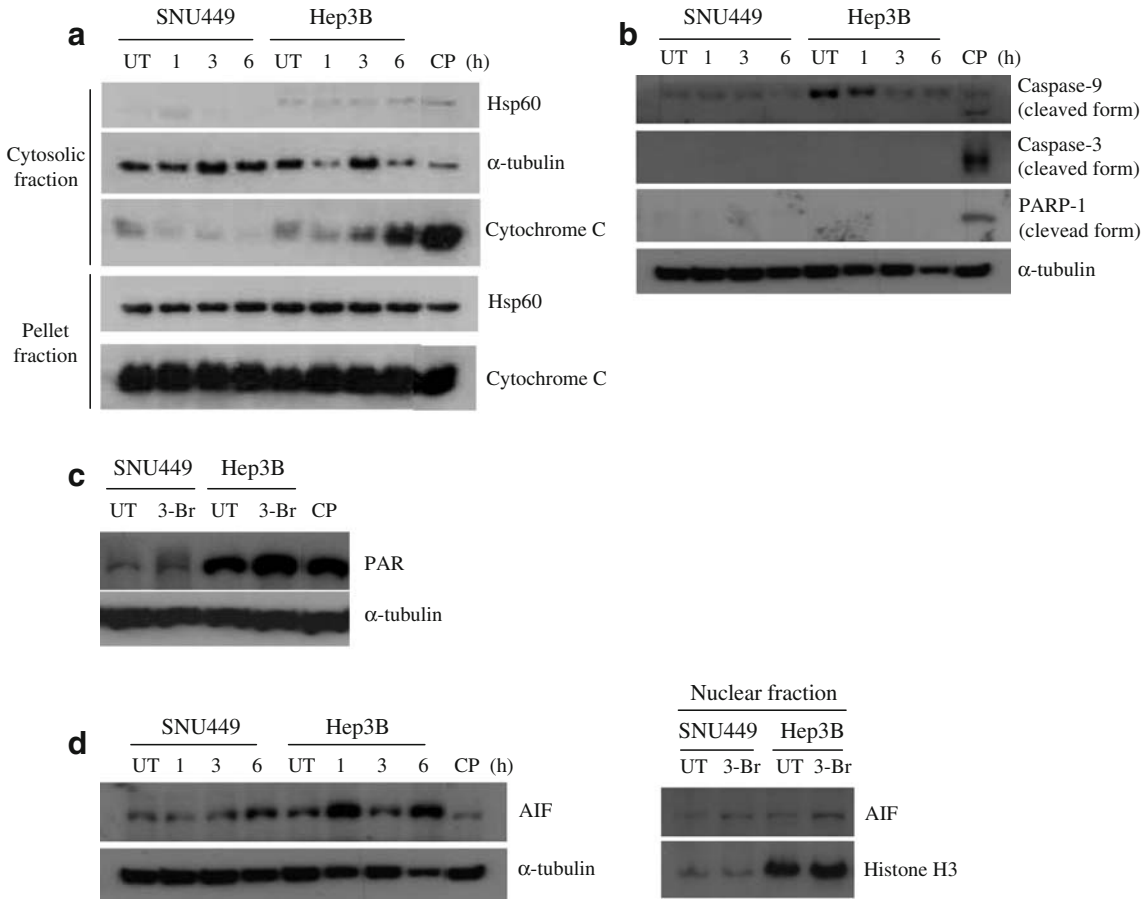

Fig. 6 The effect of 3-BrPA on activation of PARP-1 and translocation of AIF to the nucleus. **a** Cells treated with 100 μM 3-BrPA were harvested at various time intervals, and cell lysates were fractionated into a cytosolic fraction and a pellet fraction containing mitochondrial proteins. Immunoblots were performed on each fraction using anti-cytochrome *c* antibody. HSP60 was used as a fractionation control, and α-tubulin was used as a loading control. **b** Total cell lysates from cells treated with 100 μM 3-BrPA were extracted at indicated time points and immunoblotted with antibodies against caspase-3, caspase-9, PARP-1 and α-tubulin. **c** Analysis of PARP-1 activation in cells treated with 3-BrPA as detected by immunoblotting with anti-PAR antibody. **d** Whole cell lysates extracted from cells treated with 100 μM 3-BrPA at indicated time intervals were immunoblotted with anti-AIF antibody (*left panel*). Western blot analysis of the nuclear fraction was performed for the examination of AIF translocation. Histone H3 was used as a nuclear marker protein control (*right panel*)

For the further study, SNU449 and Hep3B cells were chosen. Hep3B cells were more sensitive to 3-BrPA than SNU449 cells. Since 3-BrPA has been known to target HK II, high expression of HK II in Hep3B cells might cause increased sensitivity to 3-BrPA.

Observations of intracellular ATP depletion and appearance of PI single-positive and PI-Annexin V dual-positive cell populations show that 3-BrPA induces cell death by both necrosis and apoptosis. However, 3-BrPA-induced apoptosis did not activate caspase-3 and was not blocked by a pan caspase inhibitor regardless of expression level of HK II in either SNU449 or Hep3B cells. These results imply that caspase-independent apoptotic mechanisms might be involved in 3-BrPA-induced cell death.

It has been reported that the mitochondrial electron transport chain is the major continuous source of cellular ROS (Vincent et al. 2005) and that the rate of mitochondrial ROS production is highly dependent upon the MMP (Korshunov et al. 1997). It is known that oxidative stress is induced by glucose deprivation, and mitochondrial associated HK activity plays an important role in preventing mitochondrial ROS generation (da-Silva et al. 2004). It was reported that transformed cells are more susceptible to glucose deprivation than untransformed cells. Glucose deprivation induces activation of transduction pathways and genes involved in neoplastic transformation (Spitz et al. 2000). A thiol reductant, NAC has been known to inhibit increased prooxidant production, activation of signal transduction pathways and genes expression involved in neoplastic transformation. It was demonstrated that NAC blocked a causal linkage between glucose deprivation-induced oxidative stress and glucose deprivation-induced cytotoxicity (Blackburn et al. 1999). It has been reported that ROS are the upstream mediators of β-carotene-induced apoptosis, which is caspase-3-independent, leading to the loss of MMP in Molt 4 cells (Prasad et al. 2006). In our

study, we also found that 3-BrPA induces both ROS generation and loss of MMP. Pretreatment of cells with NAC for 1 h dramatically inhibited intracellular ROS production, the loss of MMP, and 3-BrPA-induced cell death in both hepatoma cell lines tested. These imply that, although 3-BrPA is known as a specific inhibitor for HKII, 3-BrPA-induced ROS production might play a dual role in cell death, either as an activator of permeability transition or as an end product in the loss of MMP in 3-BrPA-mediated caspase-independent cell death.

Release of cytochrome *c* from the mitochondria to the cytosol is critical for inducing a permeability transition leading to apoptosis (Kroemer and Reed 2000). In our study, we found that 3-BrPA induces the efflux of cytochrome *c* to the cytosol implying the mitochondrial dysregulation. Although 3-BrPA increased intracellular ROS production in a time-dependent manner leading to the loss of MMP and cytochrome *c* release, it did not activate the mitochondria-associated caspases, caspase-9 and -3, suggesting that 3-BrPA-induced caspase-independent apoptosis might not activate the apoptosome containing caspase-9, Apaf-1, cytochrome *c*, and ATP. It was demonstrated that oxidative stress induces caspase-independent apoptosis and activates PARP-1 and AIF in RGC-5 retinal ganglion cells (Li and Osborne 2008). It was also reported that AS_2O_3-induced apoptosis in human cervical carcinoma cells induced caspase-independent translocation of AIF from the mitochondria to the nucleus (Kang et al. 2004). Since it is known that ROS-induced DNA damage activates PARP-1 leading to PAR formation, and PARP-1 hyperactivation is known to promote mitochondrial dysregulation leading to release of AIF from mitochondria to the nucleus (Xu et al. 2006), we investigated whether PAR formation and the translocation of AIF from the mitochondria to the nucleus was induced by 3-BrPA. 3-BrPA did induce PAR formation and increased the total level of AIF as well as promote the translocation of AIF from the mitochondria to the nucleus. Taken together, these results suggest that 3-BrPA-mediated cell death might require the following signaling pathway—ATP depletion, ROS production, loss of MMP, PARP-1 hyperactivation and AIF translocation.

In this study, we identified an essential role of ROS in 3-BrPA-induced cell death regardless of the expression level of HK II in hepatoma cells. To identify the possible molecular mechanism of 3-BrPA-induced cell death, we investigated the effect of 3-BrPA on cell death in hepatoma cells according to the expression level of HK II (low expression in SNU449 and high expression in Hep3B). Based on our data, we suggest that mitochondrial dysregulation by 3-BrPA-mediated ROS accumulation plays a critical role in cell death induced by 3-BrPA. Although mitochondrial dysregulation causes ATP depletion-dependent necrosis, it is also involved in the regulation of apoptotic cell death by mechanisms of activation that include PAR and translocation of AIF in the hepatoma cell lines used in this study. Thus, 3-BrPA in combination with other clinical applications can be considered as potential therapeutic options for treating aggressive tumors expressing HK II.

Acknowledgment This work was supported by the Korea Science and Engineering Foundation (KOSEF) grant funded by the Korea government (MOST) (No. R13-2002-054-05003-0).

References

Adrain C, Creagh EM, Martin SJ (2001) Embo J 20:6627–6636
Blackburn RV, Spitz DR, Liu X, Galoforo SS, Sim JE, Ridnour LA, Chen JC, Davis BH, Corry PM, Lee YJ (1999) Free Radic Biol Med 26:419–430
Chang JM, Chung JW, Jae HJ, Eh H, Son KR, Lee KC, Park JH (2007) Acad Radiol 14:85–92
da-Silva WS, Gomez-Puyou A, de Gomez-Puyou MT, Moreno-Sanchez R, De Felice FG, de Meis L, Oliveira MF, Galina A (2004) J Biol Chem 279:39846–39855
Foubister V (2002) Drug Discov Today 7:934–935
Geschwind JF, Ko YH, Torbenson MS, Magee C, Pedersen PL (2002) Cancer Res 62:3909–3913
Geschwind JF, Georgiades CS, Ko YH, Pedersen PL (2004) Expert Rev Anticancer Ther 4:449–457
Gwak GY, Yoon JH, Kim KM, Lee HS, Chung JW, Gores GJ (2005) J Hepatol 42:358–364
Higuchi Y (2004) J Cell Mol Med 8:455–464
Kakkar P, Singh BK (2007) Mol Cell Biochem 305:235–253
Kang YH, Yi MJ, Kim MJ, Park MT, Bae S, Kang CM, Cho CK, Park IC, Park MJ, Rhee CH, Hong SI, Chung HY, Lee YS, Lee SJ (2004) Cancer Res 64:8960–8967
Kim JS, Lee JM, Chwae YJ, Kim YH, Lee JH, Kim K, Lee TH, Kim SJ, Park JH (2004) Biochem Pharmacol 67:1459–1468
Kim W, Yoon JH, Jeong JM, Cheon GJ, Lee TS, Yang JI, Park SC, Lee HS (2007) Mol Cancer Ther 6:2554–2562
Ko YH, Pedersen PL, Geschwind JF (2001) Cancer Lett 173:83–91
Ko YH, Smith BL, Wang Y, Pomper MG, Rini DA, Torbenson MS, Hullihen J, Pedersen PL (2004) Biochem Biophys Res Commun 324:269–275
Korshunov SS, Skulachev VP, Starkov AA (1997) FEBS Lett 416:15–18
Kroemer G, Reed JC (2000) Nat Med 6:513–519
Lemasters JJ (2005) Gastroenterology 129:351–360
Li GY, Osborne NN (2008) Brain Res 1188:35–43
Mathupala SP, Rempel A, Pedersen PL (1995) J Biol Chem 270:16918–16925
Mathupala SP, Ko YH, Pedersen PL (2006) Oncogene 25:4777–4786
McEligot AJ, Yang S, Meyskens FL Jr (2005) Annu Rev Nutr 25:261–295
Otera H, Ohsakaya S, Nagaura Z, Ishihara N, Mihara K (2005) Embo J 24:1375–1386
Park JG, Lee JH, Kang MS, Park KJ, Jeon YM, Lee HJ, Kwon HS, Park HS, Yeo KS, Lee KU et al (1995) Int J Cancer 62:276–282
Pastorino JG, Hoek JB, Shulga N (2005) Cancer Res 65:10545–10554
Prasad V, Chandele A, Jagtap JC, Sudheer Kumar P, Shastry P (2006) Free Radic Biol Med 41:431–442
Spitz DR, Sim JE, Ridnour LA, Galoforo SS, Lee YJ (2000) Ann N Y Acad Sci 899:349–362
Ueda S, Masutani H, Nakamura H, Tanaka T, Ueno M, Yodoi J (2002) Antioxid Redox Signal 4:405–414

Vali M, Liapi E, Kowalski J, Hong K, Khwaja A, Torbenson MS, Georgiades C, Geschwind JF (2007) J Vasc Interv Radiol 18:95–101
van Wijk SJ, Hageman GJ (2005) Free Radic Biol Med 39:81–90
Vincent AM, McLean LL, Backus C, Feldman EL (2005) FASEB J 19:638–640
Xu RH, Pelicano H, Zhou Y, Carew JS, Feng L, Bhalla KN, Keating MJ, Huang P (2005) Cancer Res 65:613–621
Xu Y, Huang S, Liu ZG, Han J (2006) J Biol Chem 281:8788–8795
Yu SW, Wang H, Poitras MF, Coombs C, Bowers WJ, Federoff HJ, Poirier GG, Dawson TM, Dawson VL (2002) Science 297:259–263